Analysis of Single and Coupled Microstrip Lines on Anisotropic Substrates Using Differential Matrix Operators and the Spectral-Domain Method

Yinchao Chen and Benjamin Beker, *Member, IEEE*

***Abstract*—In this paper, a differential matrix operator technique is presented to simplify the formulation of boundary-value problems for open millimeter-wave integrated circuits (MIC's) which use anisotropic substrates. The spectral-domain method is applied to analyze the propagation characteristics of single and coupled microstrip lines printed on anisotropic substrates whose properties are described by both $[\varepsilon]$ and $[\mu]$ tensors. In addition to considering the permittivity and permeability as a uniaxial or biaxial tensor, the effects of coordinate misalignment between the principal axes of $[\varepsilon]$ and those of the structure in the transverse plane are also included. It is shown that the misalignment in $[\varepsilon]$ and the presence of the $[\mu]$ tensor has a significant effect on the dispersive properties of these two structures.**

I. Introduction

In RECENT years, the use of anisotropic materials as microwave and millimeter-wave substrates has become popular, [1]–[4] primarily due to their advantages over isotropic substrates in the development of a variety of devices, including directional couplers and microstrip antennas. In addition, from practical standpoint, this topic is also important because even isotropic MIC substrates may exhibit anisotropic properties at higher millimeter-wave frequencies. However, until now, most of the emphasis was primarily given to substrate materials characterized by permittivity tensor only, and mathematical tools for their analysis were mostly limited to classical vector methods which are extremely lengthy and complicated.

To simplify the formulation of boundary-value problems involving plane wave propagation in, and reflection from, stratified anisotropic media at optical frequencies, Berreman [5] presented a 4×4 matrix formulation. This approach treats every vector quantity as well as all vector differential operators as matrices, and allows for manipulating Maxwell's equations using matrix algebra. Berreman's technique uses the so-called four-component approach (i.e., two components of the E- and two components of H-field) which reduces the vector forms of Maxwell's equations in a planar region to the solution of first order differential equations. For microwave and millimeter-wave integrated circuits, the 4×4 matrix method was adapted for use in the spectral-domain as well [6]. The Green's function was derived using the Fourier-transformed matrix method for a line source at an interface of a grounded multi-layered anisotropic substrate for both open and closed planar regions. However, no numerical results for open structures were provided.

In this paper, a general differential matrix operator technique is presented to formulate problems for open single and coupled microstrip transmission lines printed on anisotropic substrates which may be characterized by tensor permittivity and permeability at the same time. The formulation of the open MIC problem on anisotropic substrates, conceptually, is similar to that commonly employed for their isotropic counterparts. By defining every vector operator in a matrix form, the differential matrix method can treat any vector differential problem directly, such as Maxwell's equations and wave equations without any difficulty. Another valuable feature of this method is its simplicity, which basically means that every vector differential operation is reduced to matrix multiplication, with matrix sizes not exceeding 3×3. As a result, the procedure leading to the governing differential equations involves matrix algebra only, rather than repeated elimination of nonessential field components. This approach is especially well-suited for problems involving anisotropic media, and is even more effective for multi-layered structures. It permits simplified mathematical manipulations of Maxwell's equations, allowing for a quick derivation of differential equations for all components of E- or H-fields, even for substrate materials that are characterized by a full $[\varepsilon]$ or $[\mu]$ tensor.

Following the conversion of Maxwell's equations to the matrix operator form, the spectral-domain approach [7] is applied to find the dispersion properties of single and coupled microstrip lines printed on anisotropic substrates. The planar region occupied by the substrate material exhibits both dielectric and magnetic anisotropy, within which Maxwell's equations reduce to a pair of fourth order differential equations for the components of the electric field that are tangential to the air-metal-substrate interface; namely $\tilde{E}_x$ and $\tilde{E}_z$ (see Fig. 1). The remaining nonvanishing components of E- and H-field are expressed in terms of $\tilde{E}_x$ and $\tilde{E}_z$, and are used to derive the dyadic spectral-domain Green's function for the structure. The dispersion characteristics or the effective dielectric constant (ε_{eff}) are calculated by applying the Galerkin method to a set of matrix equations relating currents on the metal strips to fields at the interface.

Numerical results obtained by this method show a good agreement with data found in references [8]–[10], thus providing the validation for the theory. Several additional numerical

Manuscript received Dec. 26, 1992; revised May 22, 1992.
The authors are with the Department of Electrical and Computer Engineering, University of South Carolina, Columbia, SC 29208.
IEEE Log Number 9204021.

TABLE I
COMMON VECTOR DIFFERENTIAL OPERATORS AND THEIR MATRIX FORMS

	Conventional Vector Operator	Matrix Operator
$\tilde{\bar{F}}$	$\left(\tilde{F}_x\hat{a}_x+\tilde{F}_y\hat{a}_y+\tilde{F}_z\hat{a}_z\right)$	$\left[\tilde{F}_x,\tilde{F}_y,\tilde{F}_z\right]^T$
$\tilde{\nabla}\tilde{\varphi}$	$\left(-j\alpha\hat{a}_x+\frac{d}{dy}\hat{a}_y-j\beta\hat{a}_z\right)$	$\left[-j\alpha,\frac{d}{dy},-j\beta\right]^T\tilde{\varphi}$
$\tilde{\nabla}\cdot\tilde{\bar{F}}$	$\left(-j\alpha\tilde{F}_x+\frac{d\tilde{F}_y}{dy}-j\beta\tilde{F}_z\right)$	$\left[-j\alpha,\frac{d}{dy},-j\beta\right]\left[\tilde{F}_x,\tilde{F}_y,\tilde{F}_z\right]^T$
$\tilde{\nabla}^2\tilde{\varphi}$	$\left(-\alpha^2+\frac{d^2}{dy^2}-\beta^2\right)\tilde{\varphi}$	$\left[-j\alpha,\frac{d}{dy},-j\beta\right]\left[-j\alpha,\frac{d}{dy},-j\beta\right]^T\tilde{\varphi}$
$\tilde{\nabla}\times\tilde{\bar{F}}$	$\begin{vmatrix}\hat{a}_x & \hat{a}_y & \hat{a}_z\\ -j\alpha & \frac{d}{dy} & -j\beta\\ \tilde{F}_x & \tilde{F}_y & \tilde{F}_z\end{vmatrix}$	$\begin{bmatrix}0 & j\beta & \frac{d}{dy}\\ -j\beta & 0 & j\alpha\\ -\frac{d}{dy} & -j\alpha & 0\end{bmatrix}\begin{bmatrix}\tilde{F}_x\\ \tilde{F}_y\\ \tilde{F}_z\end{bmatrix}$

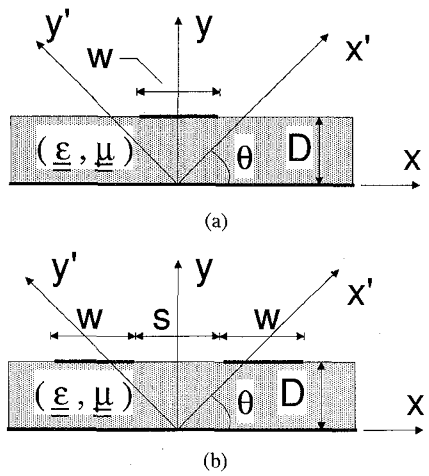

Fig. 1. Geometry of open microstrip transmission lines: (a) single, (b) coupled.

case-studies are performed to show that the misalignment between the coordinate system of the permittivity tensor with that of the guiding structure has a measurable degree of influence on the propagation properties of the transmission line. Finally, effects on the effective index of refraction $(n_{eff})^2 = (\beta/k_o)^2$ due to the presence of anisotropic characteristics in the $[\mu]$ tensor are examined as well.

II. DIFFERENTIAL MATRIX OPERATORS

Manipulation of Maxwell's equations primarily involves three vector differential operators; namely, the gradient, divergence, and curl. In order to aid the formulation of the microstrip (or planar region) boundary-value problem, Maxwell's equations are Fourier transformed to the spectral-domain using the following integral:

$$\tilde{\Phi}(\alpha, y, \beta) = \int_{-\infty}^{\infty} \Phi(x, y)e^{+j(\alpha x-\beta z)}\, dx, \tag{1}$$

where Φ can be any component of the electric or magnetic field. Using the above defined transform intergal, the differential vector operators can be transformed to the spectral-domain well. Table I gives a compact summary of common vector operators which appear in Maxwell's equations, along with their equivalent differential matrix forms. In this table, quantities $\tilde{\varphi}$ and $\tilde{\boldsymbol{F}}$ are scalar and vector functions of position along the direction perpendicular to the inhomogeneity (see Fig. 1).

If the substrate material is characterized by the following forms of the permittivity and permeability tensors

$$\varepsilon_0[\varepsilon] = \varepsilon_0 \begin{bmatrix} \varepsilon_{xx} & \varepsilon_{xy} & 0 \\ \varepsilon_{yx} & \varepsilon_{yy} & 0 \\ 0 & 0 & \varepsilon_{zz} \end{bmatrix} \tag{2a}$$

$$\mu_0[\mu] = \mu_0 \begin{bmatrix} \mu_{xx} & 0 & 0 \\ 0 & \mu_{yy} & 0 \\ 0 & 0 & \mu_{zz} \end{bmatrix}, \tag{2b}$$

then with the help of matrix operators defined above, Maxwell's equations in the spectral-domain can be rewritten as

$$\begin{bmatrix} 0 & +j\beta & d/dy \\ -j\beta & 0 & j\alpha \\ -d/dy & -j\alpha & 0 \end{bmatrix} \begin{bmatrix} \tilde{E}_x \\ \tilde{E}_y \\ \tilde{E}_z \end{bmatrix} = -j\omega\mu_0 \begin{bmatrix} \mu_{xx} & 0 & 0 \\ 0 & \mu_{yy} & 0 \\ 0 & 0 & \mu_{zz} \end{bmatrix} \begin{bmatrix} \tilde{H}_x \\ \tilde{H}_y \\ \tilde{H}_z \end{bmatrix} \tag{3}$$

$$\begin{bmatrix} 0 & +j\beta & d/dy \\ -j\beta & 0 & j\alpha \\ -d/dy & -j\alpha & 0 \end{bmatrix} \begin{bmatrix} \tilde{H}_x \\ \tilde{H}_y \\ \tilde{H}_z \end{bmatrix} = j\omega\varepsilon_0 \begin{bmatrix} \varepsilon_{xx} & \varepsilon_{xy} & 0 \\ \varepsilon_{yx} & \varepsilon_{yy} & 0 \\ 0 & 0 & \varepsilon_{zz} \end{bmatrix} \begin{bmatrix} \tilde{E}_x \\ \tilde{E}_y \\ \tilde{E}_z \end{bmatrix}. \tag{4}$$

The two corresponding vector wave equations in a planar anisotropic medium, characterized by $[\varepsilon]$ and $[\mu]$ of (2), can be readily shown to have the following forms:

$$\{[\tilde{\nabla}\times][\mu]^{-1}[\tilde{\nabla}\times] - k_o^2[\varepsilon]\}[\tilde{E}] = [0] \tag{5a}$$

$$\{[\tilde{\nabla}\times][\varepsilon]^{-1}[\tilde{\nabla}\times] - k_o^2[\mu]\}[\tilde{H}] = [0], \tag{5b}$$

where $[\tilde{E}] = [\tilde{E}_x, \tilde{E}_y, \tilde{E}_z]^T$ and $[\tilde{H}] = [\tilde{H}_x, \tilde{H}_y, \tilde{H}_z]^T$. Either one of the matrix wave equations (5a) or (5b) can now be reduced to the three coupled, second order differential equations for the components of $\boldsymbol{E}$ or $\boldsymbol{H}$. By comparison, the series of matrix operations needed to solve relations (5) are simpler than corresponding conventional vector operations which are required to achieve the same goal.

III. The Dyadic Green's Function

Both single and coupled microstrip lines, which are shown in Fig. 1, consist of a thin anisotropic layer characterized by $[\varepsilon]$ and $[\mu]$ tensors simultaneously. The grounded anisotropic substrate of thickness D, is assumed to be lossless and is infinite in the x and z directions, having infinitesimally thin and perfectly conducting metal strips printed on its top. The dielectric permittivity tensor is diagonal in the coordinate system of its principal axes (x', y', z') with $(\varepsilon_{\eta\eta}, \varepsilon_{\xi\xi}, \varepsilon_{\zeta\zeta})$ being the corresponding tensor elements. If the coordinates of the guiding structure (x, y, z) are misaligned with those of the material, then $[\varepsilon]$ will have all of its elements given by the ensuing relations

$$\varepsilon_{xx} = \varepsilon_{\eta\eta}\cos^2\theta + \varepsilon_{\xi\xi}\sin^2\theta \tag{6a}$$
$$\varepsilon_{yy} = \varepsilon_{\eta\eta}\sin^2\theta + \varepsilon_{\xi\xi}\cos^2\theta \tag{6b}$$
$$\varepsilon_{xy} = (\varepsilon_{\eta\eta} - \varepsilon_{\xi\xi})\sin\theta\cos\theta \tag{6c}$$
$$\varepsilon_{yx} = \varepsilon_{xy} \tag{6d}$$
$$\varepsilon_{zz} = \varepsilon_{\zeta\zeta} \tag{6e}$$

where θ is the misalignment angle also shown in Fig. 1. On the other hand, the permeability tensor of the substrate is assumed to be diagonal throughout the remainder of this paper.

Next, (5a) is used to obtain two second order, coupled differential equations for the tangential (to the air-substrate interface) components of electric field which after simplification will have the following form:

$$a_0\frac{d^2\tilde{E}_x}{dy^2} + ja_1\frac{d\tilde{E}_x}{dy} + a_2\tilde{E}_x + b_0\frac{d^2\tilde{E}_z}{dy^2} + jb_1\frac{d\tilde{E}_z}{dy} + b_2\tilde{E}_z = 0 \tag{7a}$$

$$c_0\frac{d^2\tilde{E}_x}{dy^2} + jc_1\frac{d\tilde{E}_x}{dy} + c_2\tilde{E}_x + d_0\frac{d^2\tilde{E}_z}{dy^2} + jd_1\frac{d\tilde{E}_z}{dy} + d_2\tilde{E}_z = 0, \tag{7b}$$

where constants a_0 through d_2 are real functions of the medium parameters, transform variable α, propagation constant β, and k_o, whose explicit forms are given in the Appendix.

Finally, by performing successive substitutions to eliminate $\tilde{E}_x$ from (7a), it is possible to obtain a decoupled, fourth order differential equation for $\tilde{E}_z$

$$w_0\frac{d^4\tilde{E}_z}{dy^4} + jw_1\frac{d^3\tilde{E}_z}{dy^3} + w_2\frac{d^2\tilde{E}_z}{dy^2} + jw_3\frac{d\tilde{E}_z}{dy} + w_4\tilde{E}_z = 0, \tag{8}$$

where the coefficients w_0 to w_4 are related to constants a_0 to d_2, as shown in the Appendix. A decoupled equation for $\tilde{E}_x$ can also be derived by following the same approach used to arrive at relation (8), and as a result, this procedure will not be repeated here.

Since the substrate is assumed to be lossless, the transverse (spectral-domain) propagation parameter, γ, is either purely real or imaginary, with values of α ranging from negative to positive infinity. Consequently, the solution to the characteristic equation (8) inside the substrate will lead to standing waves which mathematically are expressed in terms of sinusoidal functions. The remaining components of $\boldsymbol{E}$ and $\boldsymbol{H}$ can be expressed in terms of $\tilde{E}_x$ and $\tilde{E}_z$ by using Maxwell's curl equations (3) and (4). Finally, when the boundary conditions are enforced at the air-metal-substrate interface, i.e., at $y = D$, the following dyadic Green's function is obtained:

$$\begin{bmatrix} \tilde{G}_{zz}(\alpha,\beta) & \tilde{G}_{zx}(\alpha,\beta) \\ \tilde{G}_{xz}(\alpha,\beta) & \tilde{G}_{xx}(\alpha,\beta) \end{bmatrix} \begin{bmatrix} \tilde{J}_z(\alpha) \\ \tilde{J}_x(\alpha) \end{bmatrix} = \begin{bmatrix} \tilde{E}_z(\alpha, D) \\ \tilde{E}_x(\alpha, D) \end{bmatrix} \tag{9}$$

where its elements are given in the Appendix as well.

In order to examine the dispersion properties of single as well as coupled microstrip transmission lines numerically, an appropriate choice for the basis functions used to expand the currents $\tilde{J}_x$ and $\tilde{J}_z$, which are flowing on the metal strips, is made to ensure that they satisfy the required edge conditions. Then a standard Galerkin method in the Fourier-domain is applied along with Parserval's theorem [7] to obtain a system of matrix equations. The determinant of this system leads to a secular equation whose roots correspond to the propagation constant β.

IV. Numerical Results

In order to verify the formulation of the problem and its numerical implementation, the effective dielectric constant of both single and coupled microstriplines is calculated and compared to previously published data [8]–[10]. The substrate materials used for validation include sapphire ($\varepsilon_{xx} = \varepsilon_{zz} = 9.4$ and $\varepsilon_{yy} = 11.6$) and boron nitride ($\varepsilon_{xx} = \varepsilon_{zz} = 5.12$ and $\varepsilon_{yy} = 3.4$), with the numerical data generated for several different combinations of physical line dimensions. As can be seen from Figs. 2 and 3, a very good agreement for frequencies ranging from 5 to 45 GHz is observed between results obtained using the method presented in this paper and those reproduced from [8] and [10].

Prior to examining effects of misalignment between coordinates of the substrate and those of the single microstripline structure, the influence of the magnetic anisotropy (in addition to the dielectric anisotropy of the substrate) on $(n_{eff})^2$ is shown in Fig. 4. The change in the effective index of refraction for a material characterized by a diagonal $[\varepsilon]$ tensor with $\varepsilon_{xx} = \varepsilon_{zz} = 9.4$ and $\varepsilon_{yy} = 11.6$, is presented as a function of

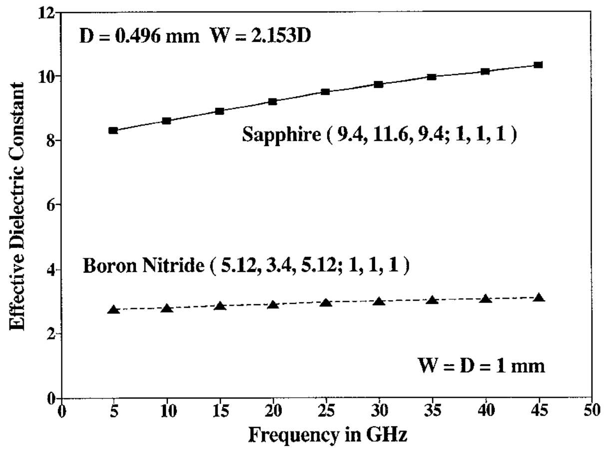

Fig. 2. Frequency dependence of ε_{eff} for a single microstrip line on sapphire or boron nitride: (—— this method, ■■■ data from [8]; - - - - - this method, △ △ △ data from [9]).

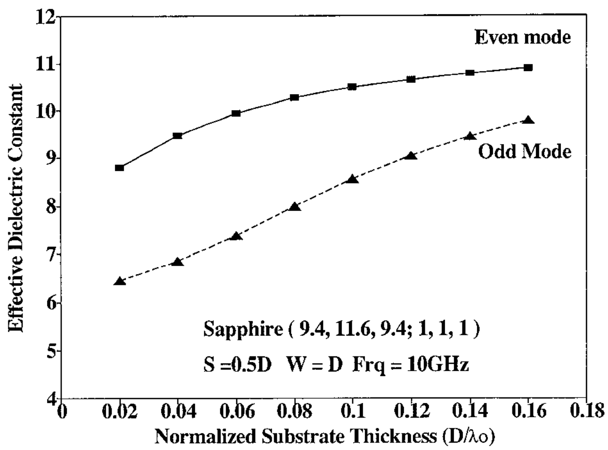

Fig. 3. ε_{eff} for even and odd modes as functions of the normalized substrate thickness (D/λ_o) for a coupled microstrip line on sapphire: (—— this method, ■■■ data from [10]; - - - - - this method, △ △ △ data from [10]).

individual elements of the permeability $(\mu_{xx}, \mu_{yy}, \mu_{zz})$ at 10 GHz. One element is allowed to vary at the time within the range of 1 to 2. It is found that the dispersion characteristics of a single microstrip are most sensitive to the variation of the μ_{xx} (or the xx) element of $[\mu]$. Notice, however, that in this case the change in $(n_{eff})^2$ is quite profound and has a nearly linear dependence over the entire range of μ_{xx}.

The same parameter study was also carried out for the coupled microstripline, but this time, with a 30 degree misalignment between (x, y, z) and (x', y', z') coordinates. As shown in Fig. 5, a similar dispersion pattern for the effective index of refraction, to that of a single microstrip, can be observed again. Once more, $(n_{eff})^2$ increases almost lineally with incremental changes in μ_{xx}. Interestingly, this behavior is seen for both the odd and even modes, with the exception that the slopes of the dispersion curves are not the same for the two cases.

Finally, the effects of coordinate misalignment for the two structures are shown in Figs. 6 and 7. The effective index of refraction and normalized guide wavelength are plotted versus the misalignment angle θ from 0 to 90 degrees (Fig. 6), whose

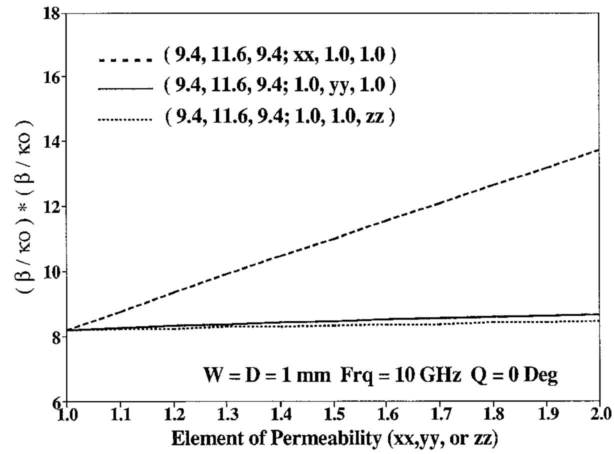

Fig. 4. $(n_{eff})^2$ as a function of element of the permeability $(\mu_{xx}, \mu_{yy},$ or $\mu_{zz})$ for a single microstrip line.

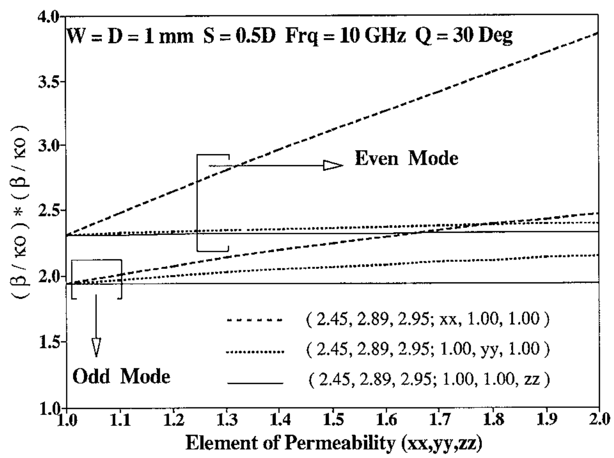

Fig. 5. $(n_{eff})^2$ for even and odd modes as a function of element of the permeability $(\mu_{xx}, \mu_{yy},$ or $\mu_{zz})$ for a coupled microstrip line.

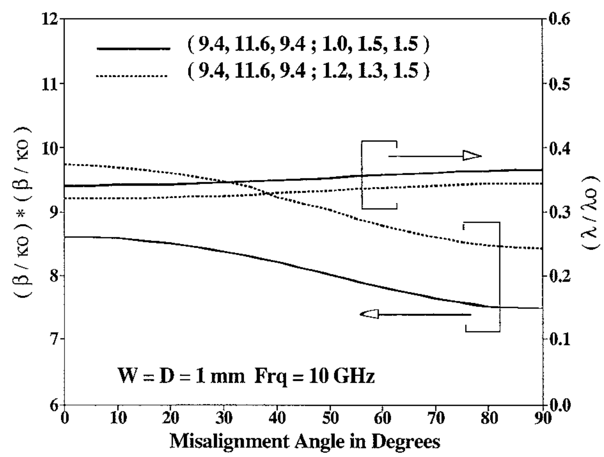

Fig. 6. $(n_{eff})^2$ and normalized guide wavelength (λ/λ_o) as a function of the misalignment angle for single microstrip line.

geometrical and medium parameters are shown in the figure. Numerical results indicate that as θ increases, $(n_{eff})^2$ decreases, while normalized guide wavelength becomes slightly larger. The same behavior can be observed for the coupled line as well, for both its odd and even modes (see Fig. 7).

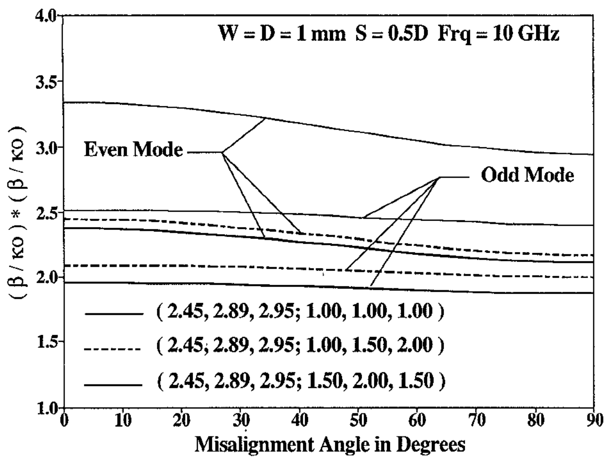

Fig. 7. $(n_{eff})^2$ for even and odd modes as a function of the misalignment angle for a coupled microstrip line.

V. Conclusion

A differential matrix operator approach in conjunction with the spectral-domain method was presented to study dispersion characteristics of open single and coupled microstrip transmission lines. It was found that converting Maxwell's equations in the Fourier-transformed domain to a matrix form simplified their manipulation in order to obtain differential equations for the tangential components of the electric field, especially when the substrate is anisotropic. Effects of both dielectric and magnetic anisotropies were examined by changing the misalignment angle between the axes of $[\varepsilon]$ and those of the structure. The influence of the anisotropic permeability tensor, in addition to the anisotropy in the permittivity, was observed to be significant, particularly for changes in μ_{xx}.

VI. Appendix

The coefficients of the coupled, second order differential equations for $\tilde{E}_x$ and $\tilde{E}_z$ appearing in (7a) and (7b) are given by

$$a_0 = \beta^2/\mu_{xx} - k_o^2\varepsilon_{yy} \quad \text{(A1)}$$
$$a_1 = \alpha k_o^2(\varepsilon_{xy} + \varepsilon_{yx}) \quad \text{(A2)}$$
$$a_2 = G_o(k_o^2\mu_{zz}\varepsilon_{xx} - \beta^2\mu_{zz}/\mu_{yy}) + k_o^4\mu_{zz}\varepsilon_{xy}\varepsilon_{yx} \quad \text{(A3)}$$
$$b_0 = -\alpha\beta/\mu_{xx} \quad \text{(A4)}$$
$$b_1 = \beta k_o^2\mu_{zz}\varepsilon_{xy}/\mu_{xx} \quad \text{(A5)}$$
$$b_2 = G_o\alpha\beta\mu_{zz}/\mu_{yy} \quad \text{(A6)}$$
$$c_0 = -\alpha\beta/\mu_{zz} \quad \text{(A7)}$$
$$c_1 = \beta k_o^2\varepsilon_{yx} \quad \text{(A8)}$$
$$c_2 = G_o\alpha\beta\mu_{xx}/\mu_{yy} \quad \text{(A9)}$$
$$d_0 = \alpha^2/\mu_{zz} - k_o^2\varepsilon_{yy} \quad \text{(A10)}$$
$$d_1 = 0 \quad \text{(A11)}$$
$$d_2 = G_o(k_o^2\mu_{xx}\varepsilon_{zz} - \alpha^2\mu_{xx}/\mu_{yy}), \quad \text{(A12)}$$

where $G_o = \beta^2/\mu_{xx} + \alpha^2/\mu_{zz} - k_o^2\varepsilon_{yy}$.

When the coupled equation set (7a) and (7b) is decoupled to obtain an independent fourth order differential equation which $\tilde{E}_z$ satisfies, the new set of constants w_0 through w_4 in (8) can be written as

$$w_0 = d_0'a_0' - b_0'c_0' \quad \text{(A13)}$$
$$w_1 = b_1'c_0' - d_1'a_0' + b_0'c_1' - d_0'a_1' \quad \text{(A14)}$$
$$w_2 = d_2'a_0' - b_2'c_0' + b_1'c_1' - d_1'a_1' \quad \text{(A14)}$$
$$w_3 = b_3'c_0' - d_3'a_0' + b_2'c_1' - d_2'a_1 \quad \text{(A15)}$$
$$w_4 = b_3'c_1' - d_3'a_1' \quad \text{(A16)}$$

with

$$a_0' = a_1 - a_0(a_2c_0 - c_2a_0)/D_o \quad \text{(A17)}$$
$$a_1' = a_2 \quad \text{(A18)}$$
$$b_0' = -a_0(b_0c_0 - d_0a_0)/D_o \quad \text{(A19)}$$
$$b_1' = b_0 + a_0(b_1c_0 - d_1a_0)/D_o \quad \text{(A20)}$$
$$b_2' = b_1 - a_0(b_2c_0 - d_2a_0)/D_o \quad \text{(A21)}$$
$$b_3' = b_2 \quad \text{(A22)}$$
$$c_0' = c_1 - c_0(a_2c_0 - c_2a_0)/D_o \quad \text{(A23)}$$
$$c_1' = c_2 \quad \text{(A24)}$$
$$d_0' = -c_0(b_0c_0 - d_0a_0)/D_o \quad \text{(A25)}$$
$$d_1' = d_0 + c_0(b_1c_0 - d_1a_0)/D_o \quad \text{(A26)}$$
$$d_2' = d_1 - c_0(b_2c_0 - d_2a_0)/D_o \quad \text{(A27)}$$
$$d_3' = d_2, \quad \text{(A29)}$$

and $D_o = c_1a_0 - a_1c_0$.

Finally, explicit expressions for the elements of the Green's function shown in equation (10) are listed below:

$$G_{zz} = j\beta\gamma_1U_0/y_1 + j\alpha V_0 \quad \text{(A30)}$$
$$G_{zx} = j\beta\gamma_1U_1/y_1 + j\alpha V_1 \quad \text{(A31)}$$
$$G_{xz} = j\alpha\gamma_1U_0/y_1 - j\beta V_0 \quad \text{(A32)}$$
$$G_{xx} = j\alpha\gamma_1U_1/y_1 - j\beta V_1 \quad \text{(A33)}$$

where $y_1 = j\omega\varepsilon_0, \gamma_1 = (\alpha^2 + \beta^2 - k_o^2)^{1/2}$, and

$$U_0 = (\beta Q_{22} - \alpha Q_{12})/\Delta_Q \quad \text{(A34)}$$
$$U_1 = (\alpha Q_{22} + \beta Q_{12})/\Delta_Q \quad \text{(A35)}$$
$$V_0 = (\alpha Q_{11} - \beta Q_{21})/\Delta_Q \quad \text{(A36)}$$
$$V_1 = -(\beta Q_{11} + \alpha Q_{21})/\Delta_Q \quad \text{(A37)}$$

with $\Delta_Q = Q_{11}Q_{22} - Q_{12}Q_{21}$, and

$$Q_{11} = B_{AA}G_1 + B_{BA}G_2 - j(\alpha^2 + \beta^2) \quad \text{(A38)}$$
$$Q_{12} = B_{AB}G_1 + B_{BB}G_2 \quad \text{(A39)}$$
$$Q_{21} = B_{AA}G_3 + B_{BA}G_4 \quad \text{(A40)}$$
$$Q_{22} = B_{AB}G_3 + B_{BB}G_4 - j\gamma_1(\alpha^2 + \beta^2)/z_1, \quad \text{(A41)}$$

where $z_1 = j\omega\mu_0$. The constants G_1 through G_4 are defined as

$$G_1 = \beta H_A - \alpha H_E + ct_a(\beta H_B - \alpha H_F) \quad \text{(A42)}$$
$$G_2 = \beta H_C - \alpha H_G + ct_b(\beta H_D - \alpha H_H) \quad \text{(A43)}$$
$$G_3 = \alpha H_A + \beta H_E + ct_a(\alpha H_B + \beta H_F) \quad \text{(A44)}$$
$$G_4 = \alpha H_C + \beta H_G + ct_b(\alpha H_D + \beta H_H) \quad \text{(A45)}$$

using the following shorthand notation $ct_a = \coth(D\gamma_a)$ and $ct_b = \coth(D\gamma_b)$, with

$$B_{AA} = j\gamma_1(\beta E_b - \alpha)/[y_1(E_b - E_a)] \quad \text{(A46)}$$
$$B_{AB} = j(\alpha E_b + \beta)/(E_b - E_a) \quad \text{(A47)}$$
$$B_{BA} = -j\gamma_1(\beta E_a - \alpha)/[y_1(E_b - E_a)] \quad \text{(A48)}$$
$$B_{BB} = -j(\alpha E_a + \beta)/(E_b - E_a). \quad \text{(A49)}$$

The remaining constants appearing the above expressions are given by

$$E_{a,b} = -[b_0\gamma_{a,b}^2 + b_2]/[a_0\gamma_{a,b}^2 + a_2] \quad \text{(A50)}$$
$$E_A = k_o^2\varepsilon_{yx}E_a/G_0 \quad \text{(A51)}$$
$$E_B = j\gamma_a(\alpha E_a/\mu_{zz} + \beta/\mu_{xx})/G_0 \quad \text{(A52)}$$
$$E_C = k_o^2\varepsilon_{yx}E_b/G_0 \quad \text{(A53)}$$
$$E_D = j\gamma_b(\alpha E_b/\mu_{zz} + \beta/\mu_{xx})/G_0 \quad \text{(A54)}$$
$$H_A = -j\beta E_A/(z_1\mu_{xx}) \quad \text{(A55)}$$
$$H_B = -(j\beta E_B + \gamma_a)/(z_1\mu_{xx}) \quad \text{(A56)}$$
$$H_C = -j\beta E_C/(z_1\mu_{xx}) \quad \text{(A57)}$$
$$H_D = -(j\beta E_D + \gamma_b)/(z_1\mu_{xx}) \quad \text{(A58)}$$
$$H_E = j\alpha E_A/(z_1\mu_{zz}) \quad \text{(A59)}$$
$$H_F = (j\alpha E_B + \gamma_a E_a)/(z_1\mu_{zz}) \quad \text{(A60)}$$
$$H_G = j\alpha E_C/(z_1\mu_{zz}) \quad \text{(A61)}$$
$$H_H = (j\alpha E_D + \gamma_b E_b)/(z_1\mu_{zz}). \quad \text{(A62)}$$

REFERENCES

[1] N. G. Alexopoulos, "Integrated-circuit structures on anisotropic substrates," *IEEE Trans. Microwave Theory Tech.*, vol. MTT-33, pp. 847–881, Oct. 1985.
[2] J. L. Tsalamengas, N. K. Uzunoglu, and N. G. Alexopoulos, "Propagation characteristics of a microstrip line printed on a general anisotropic substrate," *IEEE Trans. Microwave Theory Tech.*, vol. MTT-33, no. 10, pp. 941–945, Oct. 1985.
[3] T. Kitazawa and T. Itoh, "Asymmetrical coplanar waveguide with finite metallization thickness containing anisotropic media," *IEEE Trans. Microwave Theory Tech.*, vol. 39, no. 8, pp. 1426–1433, Aug. 1991.
[4] C. M. Krowne, "Green's function in the spectral domain for biaxial and uniaxial anisotropic planar dielectric structures," *IEEE Trans. Antennas Propagat.*, vol. AP-32, pp. 1273–1281, Dec. 1984.
[5] D. W. Berreman, "Optics in stratified and anisotropic media: 4 × 4-matrix formulation," *J. Opt. Soc. Am.*, vol. 62, no. 4, pp. 502–510, Apr. 1972.
[6] C. M. Krowne, "Fourier transformed matrix method of finding propagation characteristics of complex anisotropic layered media," *IEEE Trans. Microwave Theory Tech.*, vol. MTT-32, no. 12, pp. 1617–1625, Dec. 1984.
[7] T. Itoh and R. Mittra, "Spectral-domain method for calculating the dispersion characteristics of microstrip lines," *IEEE Trans. Microwave Theory Tech.*, vol. MTT-21, pp. 496–499, July 1973.
[8] M. Maia, A. D'Assuncao, and A. Giarola, "Dynamic analysis of microstrip lines and finlines on uniaxial anisotropic substrates," *IEEE Trans. Microwave Theory Tech.*, vol. MTT-35, pp. 881–886, Oct. 1987.
[9] M. Geshiro, S. Yagi, and S. Sawa, "Analysis of slotlines and microstrip lines on anisotropic substrates," *IEEE Trans. Microwave Theory Tech.*, vol. 39, pp. 64–69, Jan. 1991.
[10] T. Kitazawa and Y. Hayashi, "Propagation characteristics of striplines with multilayered anisotropic media," *IEEE Trans. Microwave Theory Tech.*, vol. MTT-31, pp. 429–433, June 1983.

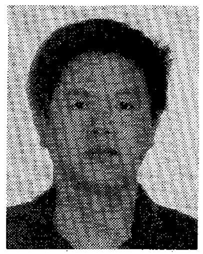

Yinchao Chen received the B.S. degree in physics from National Wuhan University, China, the M.S.E.E. degree from the University of Science and Technology of China and Nanjing Research Institute of Electronics Technology, and the Ph.D. degree in electrical engineering from the University of South Carolina, in 1982, 1985, and 1992, respectively.

From 1982 to 1988, he was with the Microwave and Antenna Laboratory, Nanjing Research Institute of Electronics Technology, as an engineer and research group leader working with design, research, and synthesis of microwave components and antennas. From 1988 to 1989, he was a research assistant in the Department of Physics, University of Tennessee, Knoxville. Since 1989, he has been with the Department of Electrical and Computer Engineering, University of South Carolina, Columbia, as a research and teaching assistant. Currently, he is a Postdoctoral Fellow in the Department, working with theory and analysis of MICs and their discontinuities. His academic interests include microwave and millimeter-wave integrated circuits, radiation, scattering, and propagation theory.

Benjamin Beker (S'83–M'88) was born in Vilnius, Lithuania, in 1959. He received the B.S.E.E., M.S.E.E., and Ph.D. degrees from the University of Illinois, Chicago, in 1982, 1984, and 1988, respectively.

From 1982 to 1988 he was a Research Assistant in the Department of Electrical Engineering and Computer Science at the University of Illinois, Chicago, working with numerically oriented scattering and radiation problems. In 1988 he joined the Department of Electrical and Computer Engineering at the University of South Carolina, Columbia, as an Assistant Professor. His research interests include EM field interaction with anisotropic materials, computational methods in scattering, radiation, and guided-wave propagation in millimeter-wave integrated circuits.